Heliyon 10 (2024) e32915

Contents lists available at ScienceDirect

Heliyon

journal homepage: www.cell.com/heliyon

Research article

# Onion husk-derived high surface area graphene-like carbon for supercapacitor electrode material application

Asel Duisenbek [a,b,*], Yerkezhan Beisenova [b,**], Renat Beissenov [b,c], Kydyr Askaruly [a,b], Mukhtar Yeleuov [a,b], Alisher Abdisattar [a,b]

[a] Satbayev University, Almaty, Kazakhstan
[b] Institute of Combustion Problems, Almaty, Kazakhstan
[c] Kazakh-British Technical University, Almaty, Kazakhstan

ARTICLE INFO

*Keywords:*
Biowaste
Carbonization
Thermochemical activation
Activated carbon
Graphene
Onion husk
Energy storage

ABSTRACT

In this study, we report the synthesis of graphene-like carbon derived from onion husk, with potential application as an electrode material in energy storage devices. Graphene-like carbon (GLC) was synthesized from onion husk (OH) by preliminary carbonization at 550 °C, followed by thermochemical activation at various temperatures to determine the optimal activation parameters. The surface morphology of graphene-like carbon from onion husk (GLC-OH) samples after carbonization shows distinct thermal exfoliation of the material. This layering upon activation in KOH promotes the formation of highly porous graphene-like carbon flakes. According to the Brunauer-Emmett-Teller (BET) method, the specific surface area at 850 °C was 1924 $m^2$/g. The X-ray diffraction (XRD) and Raman spectroscopy results reveal the emergence of few-layer graphene with a significant amount of structural defects at 850 °C. As the temperature increases, the formation shifts towards multilayer graphene, which leads to a decrease in the specific surface area of the carbon material. The electrochemical characterization of the assembled GLC–OH–based supercapacitor synthesized at 850 °C revealed a markedly higher specific capacitance value of 131 F/g, along with a Coulombic efficiency of 98 % at a gravimetric current density of 1 A/g. Additionally, it exhibited a low charge transfer resistance ($R_{CT}$) of approximately 1.4 Ω.

Our study investigates the influence of structural changes on the electrochemical performance of biomass-derived activated carbon, highlighting the potential of graphene-like carbon from onion husk as a promising and low-cost material for future energy storage devices.

## 1. Introduction

In recent years, the number of environmentally friendly energy storage solutions has increased significantly. Supercapacitors, recognized as advanced electrochemical energy storage devices, demonstrate significant promise and potential to meet the rapidly growing energy storage demands. Unlike conventional types of batteries, supercapacitors accumulate energy through the reverse adsorption of charged ions at the electrode/electrolyte interface, resulting in quick charge and discharge cycles with high power

* Corresponding author. Satbayev University, Almaty, Kazakhstan.
** Corresponding author.
*E-mail addresses:* aselka_star@mail.ru (A. Duisenbek), mamyrbayeva.e@gmail.com (Y. Beisenova).

https://doi.org/10.1016/j.heliyon.2024.e32915
Received 17 November 2023; Received in revised form 3 June 2024; Accepted 12 June 2024
Available online 13 June 2024
2405-8440/© 2024 The Authors. Published by Elsevier Ltd. This is an open access article under the CC BY-NC license (http://creativecommons.org/licenses/by-nc/4.0/).

density. However, the way to enhance supercapacitor performance lies in the development of advanced electrode materials with exceptional electrochemical properties [1–4].

Graphene, a two-dimensional material made of carbon atoms, exhibits high electrical conductivity, chemical stability, and an extremely high specific surface area of about 2630 $m^2/g$ making it a promising material in the energy sector, particularly for electrochemical energy storage devices. However, the use of graphene is limited by the high cost of production and the difficulty of producing high-quality material on a large scale. At the same time, graphene-like materials have properties that can be similar or even superior to those of pure graphene. Currently, various types of biomass are used to obtain graphene-like carbon materials [5,6].

Carbon materials obtained from various types of biomass, such as rice husks [7,8] walnut shells [9], bamboo waste [10,11], tea waste [12], jute fibers [13], pine cones [14], coffee powder waste [15], coconut shells [16], banana peel [17], and corn grains [18], have been used to create supercapacitors, showcasing the potential of sustainable materials in this field.

Carbon materials derived from onion husks represent an attractive and sustainable alternative in the field of functional carbon materials. Onion husks, typically disregarded and disposed of as agricultural byproducts, offer a valuable opportunity for the efficient utilization of their inherent carbon content. Global onion production figures can fluctuate from year to year due to various factors, including weather conditions, market demand, and agricultural practices. However, annual production estimates for yellow onions, one of the most widely grown varieties globally, typically range from 90 to 100 million metric tons. In contrast, global production of red onion is significantly lower, estimated at around 15–20 million metric tons annually, about one-fifth of that of yellow onions.

The weight portion of onion husk, also known as onion skin or outer layers, can vary depending on the size and type of onion. Generally, onion husk constitutes a significant percentage of the total weight of an onion. On average, the weight proportion of onion husk within an onion can range from approximately 10 %–25 % of the total weight.

*Mehare* et al. [19] obtained porous carbon from onion peel without physical-chemical activation or an inert atmosphere. However, this approach did not fully allow to fully utilize the potential of onion husk, resulting in poor specific capacitance performance in supercapacitors, with a maximum capacitance value of 98 F/g at a current density of 0.1 A/g in a 1 M $H_2SO_4$ electrolyte solution. In another study [20], researchers synthesized activated carbon from red onion skin with a high specific surface area (over 3000 $m^2/g$). However, their method involved multiple steps (hydrothermal carbonization => pre-carbonization => pre-activation), which leaded to increased costs and lower mass yield of the carbon. In a two-electrode cell, the specific capacitance at a current density of 1 A/g was found not to be superior: 61 F/g for OPACs-600 °C, 67 F/g for OPACs-700 °C, and 77 F/g for OPACs-800 °C. In this research [21], activated carbon was produced from red onion skin through pre-carbonization at 450 °C for 3 h followed by thermochemical activation using KOH (at a ratio of 1:3) at 900 °C for 1 h. Under these synthesis conditions, the specific surface area of the resulting activated carbon was less than 1900 $m^2/g$, with a specific capacitance of 64 F/g at 0.1 A/g in supercapacitors.

Several studies have demonstrated higher capacitance values when using a three-electrode cell setup [19–21]. In a study [22], it was found that a three-electrode cell typically yields about twice the capacity compared to a two-electrode cell. While the enhanced sensitivity of the three-electrode configuration is advantageous for investigating faradaic reactions and interfacial processes on individual electrodes, it may introduce considerable inaccuracies when evaluating the energy storage capacity of electrode materials intended for use in ultracapacitors.

Carbonization and thermochemical activation of biomass represent simple and energy-efficient methods for producing activated carbon. This approach requires minimal resources and equipment, making it feasible for scaling up to larger production volumes. The resultant carbon possesses a graphene-like structure and exhibits a high specific surface area making it suitable for a wide range of applications.

In this study, we synthesized graphene-like carbon structures from onion husks through carbonization and thermochemical activation processes. We systematically investigated the influence of the activation temperature on the morphological structures of the graphene-like carbon and its electrochemical properties as an active material in supercapacitors.

## 2. Experimental

### 2.1. Materials and reagents

Yellow onion husk (obtained from the local market of Almaty, Kazakhstan), argon gas (Ikhsan Techno Gas, 99.99 %), potassium hydroxide (KOH, Sigma Aldrich, 85 %), carbon black (MTI Corporation), 1-Methyl-2-pyrrolidinone (NMP, Sigma Aldrich, 99 %), polyvinylidene fluoride (PVDF, MTI Corporation), nickel foil (MTI Corporation).

### 2.2. Synthesis of graphene-like porous carbon from onion husk

The original precursor, onion husk (OH), was grown on a farm in the Almaty region. Cleaning took place with hot distilled water to remove contaminants. The peeled husks were then ground in a zirconium mortar to a powdery mass and dried in an oven at 120 °C for 8 h. A two-step synthesis of graphene-like carbon was carried out as follows: 1) in the first step, carbonized onion husks (COH) were prepared in a horizontal tube furnace. The furnace was heated from room temperature to 550 °C at a heating rate of 7 °C/min and maintained at this temperature for 100 min in an argon atmosphere. After the process pyrolysis carbonization process of onion husks, the yield of the carbon product was 27.5 % by weight; 2) in the second step, graphene-like carbon was produced via chemical activation. KOH was added to the resulting COH at a mass ratio of 1:4, followed by heating to temperatures of 600 °C, 850 °C, or 950 °C for 90 min each. The inert gas (Ar) purging rate was maintained at 450 $cm^3$/min. Achieving a neutral pH level for GLC-OH was accomplished through repeated washing with hot distilled water followed by drying in an oven at 100 °C for 10 h. After

thermochemical activation, the yield of activated carbon from onion husk reached 8.4 % by weight.

### 2.3. Materials characterization

The samples of activated OH have been studied by several informative techniques. The surface morphology of the GLC samples' was investigated using JEOL JSM-6490 LA scanning electron microscopy. X'Pert MPD PRO X-ray diffractometer with Cu Kα radiation source was used for the study of the crystal structure of GLC-OH. The structure of GLC-OH was studied using an NTEGRA Raman spectrometer, which has a signal region of 80 nm in diameter using a blue 473 nm laser. Determination of the specific surface area of the PDS-OA sample: nitrogen adsorption/desorption was measured at 77 K using a gas adsorption analyzer SORBTOMETER-M (KATAKON).

### 2.4. Characterization of electrochemical properties

The electrode material was prepared by mixing onion husk-activated carbon, electrically conductive soot, and polyvinylidene fluoride (PVDF) in a 70:20:10 ratio. To obtain a suspension, 4 ml of N-methyl-2-pyrrolidone (NMP) solvent was added to 1 g of the mixed powder. The resulting mixture was then applied to 1 square centimeter of nickel foil and dried in hot air (ShS-80, Belarus) at 130 °C for 10 h. Electrochemical measurements were performed using an Elins P-40X (FRA-24 M, Russia) potentiostat galvanostat. Various scan rates were used for cyclic voltammetry (CV) data acquisition and various specific currents for galvanostatic discharge (GCD) measurements. A frequency range of 100 kHz to 10 mHz was applied for electrochemical impedance spectroscopy (EIS) measurements.

## 3. Results and discussions

### 3.1. Structural and morphological characterization

Fig. 1 (a) shows the SEM microstructure of the carbonized onion husk at 550 °C, on Fig. 1. (b, c, d) activated onion husk at 600 °C, 850 °C, and 950 °C in KOH, respectively. 2D layered carbon with different thicknesses and porosity have been observed for all activated samples. The most developed active surface with many open pores, as well as high-quality layers of sp2-hybridized graphene-like carbon, belongs to the sample activated at 850 °C. Moreover, the detailed SEM investigation of microstructure GLC-OH at 850 °C shows the formation of high-quality double-layer graphene stripes (Fig. 1e). They exhibit a similar interconnected graphene-like structure, and many pores can be observed on ultra-thin nanosheets. The morphology of the carbonized GLC-OH sample has a larger specific area of charge accumulation and conversion compared to Fig. 1a, which has a thick sheet structure (Fig. S3).

The morphology differences in carbonized and activated GLC-OH samples are mainly associated with the effect of two-dimensional separation of the band structure due to the process of high-temperature activation. Separation of flakes of two-dimensional carbon is more observed for the sample activated at 850 °C, compared to 950 °C, which is also confirmed by Raman spectroscopy. An increase in the activation temperature leads to the graphitization of the structure and a decrease in the intensity of two-dimensional carbon structures [21].

Analysis of the composition of activated carbon GLC-OH 850 °C, carried out using the EDAX method, showed that it contains a high

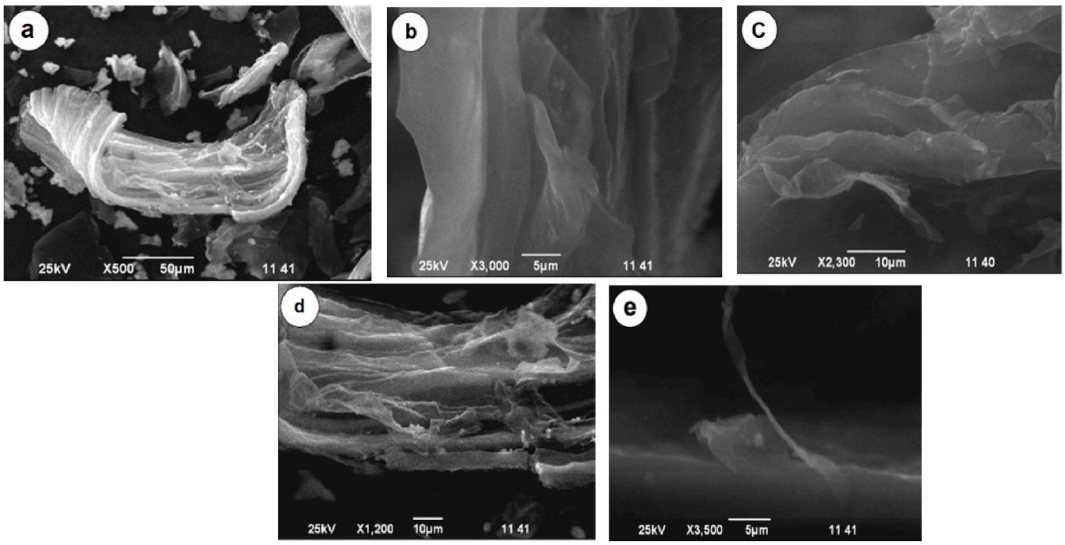


**Fig. 1.** SEM images of (a) COH, (b, c, d) GLC-OH 600 °C; 850 °C; 950 °C and (e) rolled graphene strip at 850 °C.

percentage of carbon (98 % by weight). Other elements such as aluminum (1.37 % wt), lutetium (0.27 % wt), and calcium (0.35 % wt) are present in much smaller quantities, less than 1 % by weight each (Fig. S4). This indicates that the chemical activation process was successful, and a good neutrality value (pH = 6) was achieved after washing.

The X-ray diffraction of an activated OH at 600 °C, 850 °C, and 950 °C is shown in Fig. 2a. X-ray diffraction patterns of activated OH samples at 600 °C, and 850 °C are almost similar, showing two broad peaks at 2θ ranges of 20–30° and 40–50°. Peaks of material crystallinity are not observed. Increasing the activation temperature to 950 °C, low-intensity crystalline peaks of graphite (002), (100), (101), (004), and (103) are observed respectively (JCPDS map no. 41–1487). A strong reflection (002) is observed at the peak position with a 2θ value of 26.58. Thus, when OH is activated at 950 °C, graphitization of the overall structure of the material is observed through the compaction of graphene-like sheets of carbon towards the formation of solid carbon [23–26].

The Raman spectra of the activated GLC-OH at 600 °C, 850 °C, and 950 °C samples are shown in Fig. 2b. The Raman spectrum of graphene should include the G band indicating the presence of $sp^2$ hybridized carbon atoms, the D band reflecting defects present in graphene, and the 2D band indicating the number of layers of graphene [27]. The Raman spectra GLC-OH activated at 600 °C are characterized by high-intensity D and G and broad 2D peaks. The D peak intensity shows a high amount of defects due to low activation energy at 600 °C to transform sp2-oriented graphene-like carbon and the structure is mostly amorphous. Raman spectra of activated OH at 850 °C and 950 °C samples are characterized by three peaks of high crystallinity: D-peak in the region of 1350 $cm^{-1}$-1360 $cm^{-1}$, G-peak in the region of 1570 $cm^{-1}$-1590 $cm^{-1}$ and 2D -peak in the region of 2708 $cm^{-1}$ (Table 1).

Therefore, the activated OH at 850 °C has higher intensity D and 2D peaks, demonstrating a high defects concentration in the structure, as well as the presence of multi-layer high-quality graphene [28,29]. Activation of onion husk with alkalis leads to the removal of impurity atoms from the 2D carbon crystal lattice, by forming defects, while leaving uniform high-quality graphene flakes [30–32].

The surface area measured by BET for carbonation at 550 °C was 49 $m^2/g$, while after thermochemical activation at 600 °C and 950 °C after thermochemical activation it was 388 $m^2/g$ and 919 $m^2/g$, respectively. The maximum surface area is observed at an activation temperature of 850 °C and is 1924 $m^2/g$, which is more than 39 times higher than the surface after carbonization [33]. Thermochemically derived graphene-like carbon from onion husk exhibits enhanced surface development and porosity compared to physically activated carbon. This increased surface density enhances the capacitive properties of the material, making it a promising choice for supercapacitor electrodes.

### 3.2. Electrochemical characteristics

To investigate the electrochemical characteristics of the obtained graphene-like carbon, two-electrode cells were fabricated as recommended in the article [22]. This allowed for a more precise determination of supercapacitor parameters for practical production purposes [34].

The study of the electrochemical characteristics of the GLC-OH material included the analysis of cyclic voltammetry (CV) curves, which are shown in Fig. 3. Notably, CV curves were obtained at various scanning rates (20, 40, 80 и 160 mV/s) for the GLC-OH sample at 850 °C had a characteristic rectangular profile, indicating its characteristic capacitive properties, in contrast to the behavior observed in the samples at 600 °C and 950 °C (Fig. 3 a, b, c). This closely matches the electrochemical performance typically associated with graphene, enhancing the promising electrochemical performance of the GLC-OH material at 850 °C.

Fig. 3d illustrates the CV curves of the electrodes with activated carbons at 600 °C, 850 °C, and 950 °C and carbonized mass at 550 °C, as well as Ni-foil based current collector. Notably, the GLC-OH 850 °C electrode demonstrates the highest capacity and the best

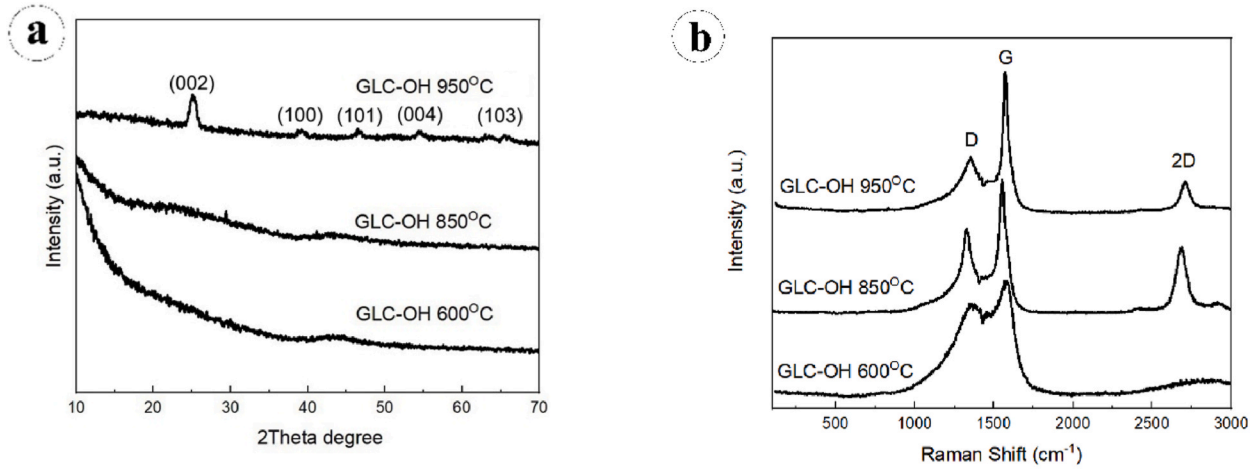


№

**Fig. 2.** The XRD (a) and Raman (b) scattering of GLC-OH 600 °C, GLC-OH 850 °C, and GLC-OH 950 °C.

**Table 1**
Comparative positions of D and G bands along with $I_D/I_G$ ratio for GLC derived from onion.

| Material | D ($cm^{-1}$) | G ($cm^{-1}$) | $I_{2D}$ | $I_D$ | $I_G$ | $I_D/I_G$ ratio | $I_{2D}/I_G$ |
|---|---|---|---|---|---|---|---|
| GLC-OH -600 °C | 1359 | 1581 | – | 2341 | 2818 | 1,2 | – |
| GLC-OH -850 °C | 1356 | 1591 | 3540 | 3939 | 4980 | 0,79 | 0,07 |
| GLC-OH -950 °C | 1353 | 1572 | 4951 | 5466 | 7266 | 0,75 | 0.07 |

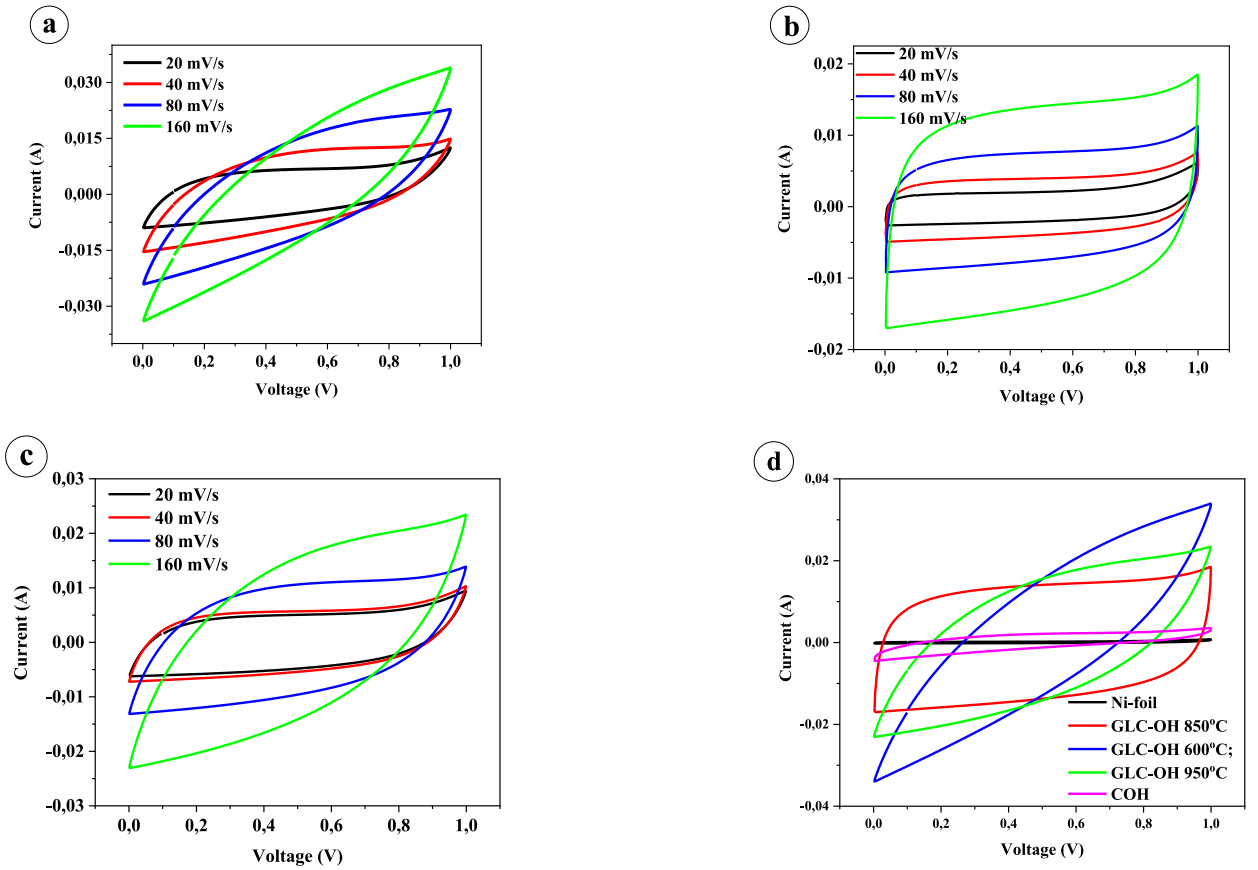


**Fig. 3.** (a) CV curves at different rates (20, 40, 80, and 160 mV/s) for GLC-OH 600 °C; (b) GLC-OH 850 $^{O}$C; (c) GLC-OH 950 °C; (d) CV curves at 160 mV/s for GLC-OH 600 °C, GLC-OH 850 °C, GLC-OH 950 °C, Ni-foil, COH.

stability whereas the shapes of CV curves of the GLC-OH 600 °C and GLC-OH 950 °C electrodes significantly deviate from rectangular shape. At the same time, both the electrode with carbonized mass and the nickel current collector exhibit practically zero capacity [35].

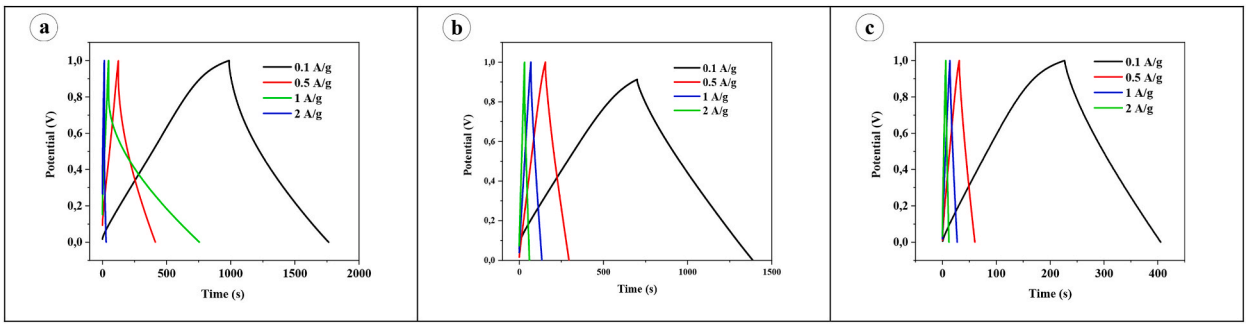


**Fig. 4.** GCD curves at 0.1, 0.5, 1, and 2 A/g current density for samples (a) GLC-OH 600 °C; (b) GLC-OH 850 °C; (c) GLC-OH 950 °C.

The galvanostatic charge-discharge (GCD) method allowed us to determine the best GLC-OH sample at 850 °C, compared to other GLC-OH samples at 600 °C and 950 °C (Fig. 4 a, b, c). Carrying out capacity studies for samples GLC-OH 600 °C, GLC-OH 850 °C, and GLC-OH 950 °C, according to charge-discharge curves at electric current values (0.1, 0.5, 1, and 2 A/g), the graphs of which are shown in Fig. 4.

The specific capacity of the obtained GLC-OH 600 °C sample was 155.19, 119, 92.56 and 56.68 F/g at current densities of 100, 500, 1000, and 2000 mA/g, the following GLC-OH 850 °C samples were 137.6, 140.1, 130.9 and 116.4 F/g at 100, 500, 1000 and 2000 mA/g and GLC-OH 950 °C were 81.1, 60.29, 54.75 and 25.2 F/g at current densities 100, 500, 1000, 2000 mA/g, respectively (Fig. 5a). Notably, the sample at 850 °C achieved the best Coulombic efficiency of 98.08 % at a current density of 1000 mA/g, while the other samples showed a Coulombic efficiency of 94.7 % and 95.3 % at the same current density for 600 °C and 950 °C samples, respectively.

In Fig. 5a for a sample with a temperature of 850 °C, the decrease in ultimate capacity was 15 %, with a 20-fold increase in current density (100 → 2000 mA/g). Conversely, for the remaining samples, GLC-OH 600 °C and GLC-OH 950 °C, a decrease in specific capacity of 63.5 % and 68.9 %, respectively, was observed.

Using the formulas given in work [36], energy density, and power density indicators were calculated, the data obtained is available in Table 2.

To gain deeper insights into how the activation temperature impacts the electrochemical characteristics of the electrodes, Electrochemical Impedance Spectroscopy (EIS) was carried out. This involved applying a voltage amplitude of 5 mV across a frequency range spanning from 100 kHz to 10 mHz, as depicted in Fig. 5b. The diameter of the semicircle observed at the higher-frequency end of these diagrams corresponds to the charge transfer resistance ($R_{CT}$) existing at the interface where the electrode interacts with the electrolyte ions [37].

At a temperature of 850 °C, the cell exhibited superior capacitance performance, as evidenced by a nearly vertical line at low frequencies, as well as a lower resistance charge transfer ($R_{CT}$) of approximately 1.4 Ω, compared to the EIS performance of onion peel-derived carbon [19]. This may have been influenced by the higher carbon content in our sample GLC-OH 850 °C (98 % by weight) according to the works [19,21] (91 % and 80 % by weight) and obtained carbon mass structure contains a graphene-like structure (see Fig. 2b).

In contrast to GLC-OH 850 °C, samples at 600 °C and 950 °C showed higher values ($R_{CT}$), about 5 Ω and 4.3 Ω, respectively. GLC-OH 950 °C electrode demonstrated better rate capability (see Fig. 5a) and conductivity than GLC-OH 600 °C due to activated carbon at 900 °C possesses higher degree of crystallinity (see Fig. 2a,b) than at 600 °C. Electrode with carbonized onion husk also demonstrated good conductivity comparable to GLC-OH 850 sample attributed to the well preserved graphite structure, but with poor ideal-capacitor like behavior. For comparison, EIS spectra of bare Ni-foil is depicted representing resistance contributed by solution and separator.

In a general context, it's crucial to note that a reduced charge transfer resistance ($R_{CT}$) typically signifies a higher specific capacitance. Specific capacitance measures a material's ability to store electrical energy per unit mass or surface area. In the case of GLC-OH 850 °C, the observed decrease in $R_{CT}$ points to improved electrical conductivity, which, in the context of electrophysics, translates to an enhanced power density when subjected to elevated current rates during charge-discharge cycles. Calculations of capacitive and diffusion-controlled contributions to charge storage for the sample GLC-OH 850 °C are provided in Fig. S2.

For supercapacitors, the long-term stability of the electrodes is also an important parameter. The stability of graphene-like carbons GLC-OH 600 °C, GLC-OH 850 °C, GLC-OH 950 °C and COH (Fig. S1 a,b) was measured by cycling up to 5000 cycles at 2 A $g^{-1}$ as shown in Fig. 5c. At 850 °C, the GLC-OH electrode showed excellent cyclic stability (<95 % capacity retention after 5000 cycles) compared to other biomass precursors used in supercapacitors [38,39].

The results show that the GLC-OH 850 °C exhibits a remarkable combination of high specific capacitance and low internal resistance, making it a promising candidate for supercapacitors. Additionally, these characteristics are comparable to, and in certain instances, surpass those of supercapacitors constructed using carbon structures derived from biological waste (Table 3).

## 4. Conclusion

Onion husk, as an active material for a supercapacitor electrode, is an attractive option due to the easy availability of onion-based

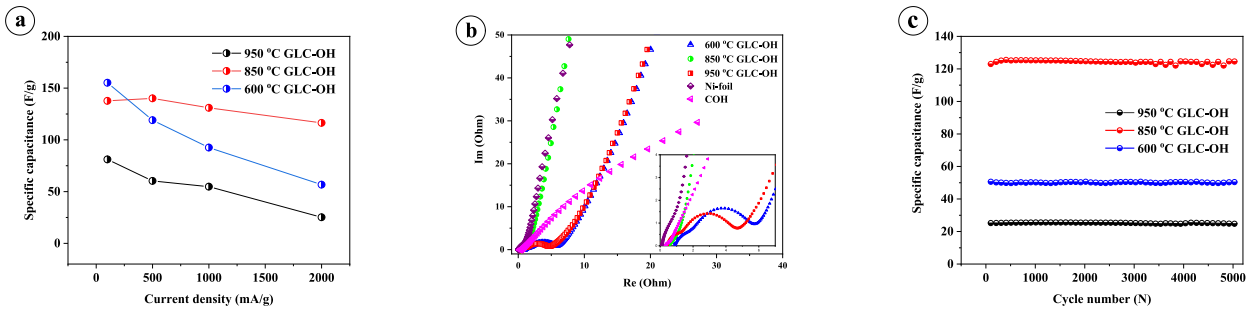


**Fig. 5.** Electrochemical performance of electrodes based on GLC-OH: (a) specific capacitance at 100, 500, 1000, and 2000 mA/g current densities; (b) EIS curve recorded in the frequency range of 100 kHz to 10 mHz; (c) cyclic stability characteristic at a constant current density of 2000 mA/g for samples GLC-OH 600 °C, GLC-OH 850 °C, GLC-OH 950 °C.

**Table 2**
Calculation result of energy density and power density at 600 °C, 850 °C, and 950 °C.

| Current density (mA/g) | Specific energy density (Wh kg $^{-1}$) | | | Specific power density (W kg $^{-1}$) | | |
|---|---|---|---|---|---|---|
| | 600 °C | 850 °C | 950 °C | 600 °C | 850 °C | 950 °C |
| 100 | 5,38 | 4,86 | 2,81 | 59.3 | 60 | 56.6 |
| 500 | 4,13 | 4,74 | 2,09 | 124 | 143 | 131 |
| 1000 | 3,21 | 4,54 | 1,9 | 249 | 280 | 214 |
| 2000 | 1,96 | 4,04 | 0,88 | 504 | 528 | 500 |

**Table 3**
Comparative performance of various activated carbon materials for supercapacitor applications.

| Biomass material | Activation reagents | Specific surface area ($m^2$ $g^{-1}$) | Application | Capacity | Electrolyte | Year | Ref. |
|---|---|---|---|---|---|---|---|
| Miscanthus | KOH | 3024 | High-performance electric double layer capacitor (EDLC) | 110,8 F/g at 1 A $g^{-1}$ | Organic | 2017 | [40] |
| Pine tree powder | KOH | 1018 | High-voltage supercapacitors | 133 F/g at 1 A $g^{-1}$ | 1 M TEABF4/ AN | 2017 | [41] |
| Jute stick | KOH | 2396 | Ultrafast supercapacitor | 131 F/g at 1 A $g^{-1}$ | 6 M KOH | 2018 | [37] |
| Coffee grounds | KOH | 1250 | Symmetric supercapacitors | 105.3 F/g | 8 M KOH | 2019 | [42] |
| Oaknut shell | KOH | 3757 | Ultra-high capacitance supercapacitors | 88 F/g at 0.5 A $g^{-1}$ | 1 M $Na_2SO_4$ | 2020 | [43] |
| Sweet corn husk | KOH | 1370 | High-voltage supercapacitors | 127 F/g | 6 M KOH | 2020 | [36] |
| Waste wood | KOH | 424 | Supercapacitors | 95 F/g | 2 mol/L KOH | 2021 | [44] |
| **Onion husk** | **KOH** | **1924** | **Symmetric supercapacitors** | **140,1 F/g at 0.5 A g−1** | **6 M KOH** | **2023** | **Present work** |

waste and excellent electrochemical performance. In this study, we used a method that allows the production of active material on a large scale with better characteristics compared to previous similar studies.

As a result of the research, it was found that graphene-like carbon obtained from onion husk waste using KOH as an activator exhibits exceptional properties that make it desirable for use in electrochemical energy storage. Graphene-like carbon derived from onion husk through thermochemical processes has yielded compelling results. The material exhibits an exceptional surface area and heightened porosity, particularly when activated at 850 °C, resulting in a maximum surface area of 1924 $m^2$/g. This superior surface structure enhances the capacitive properties of the electrode material, positioning it as a promising candidate for applications in supercapacitors and energy storage devices. Cells obtained from samples 600 °C, 850 °C, and 950 °C with two electrodes showed different results in terms of specific capacitance, however, the best values of 131 F/g at a specific current of 1 A/g corresponded to a temperature of 850 °C. The GLC-OH 850 °C supercapacitor demonstrated outstanding cyclic stability, maintaining specific capacitance after 5000 charge-discharge cycles in the potential range of 0–1 V. Furthermore, the electrochemical analyses, including cyclic voltammetry and charge-discharge studies, have showcased the exceptional performance of GLC-OH 850 °C, indicating its potential for energy storage technologies. These findings underscore the significance of thermochemical synthesis in tailoring carbon materials for electrochemical applications and open opportunities for further research.

## CRediT authorship contribution statement

**Asel Duisenbek:** Visualization, Validation, Methodology, Conceptualization. **Yerkezhan Beisenova:** Investigation, Funding acquisition. **Renat Beissenov:** Supervision, Formal analysis. **Kydyr Askaruly:** Validation, Investigation, Conceptualization. **Mukhtar Yeleuov:** Validation, Formal analysis. **Alisher Abdisattar:** Validation, Formal analysis.

## Declaration of competing interest

The authors declare that they have no known competing financial interests or personal relationships that could have appeared to influence the work reported in this paper.

## Acknowledgments

This work was supported by the Ministry of Education and Science of the Republic of Kazakhstan through the project AP15473245. The authors acknowledge Azat Seitkhan, and Renata Nemkayeva for their technical assistance in the laboratory.

## Appendix A. Supplementary data

Supplementary data to this article can be found online at https://doi.org/10.1016/j.heliyon.2024.e32915.

## References


[1] D.P. Dubal, O. Ayyad, V. Ruiz, P. Gómez-Romero, Hybrid energy storage: the merging of battery and supercapacitor chemistries, Chem. Soc. Rev. 44 (2015) 1777–1790, https://doi.org/10.1039/C4CS00266K.

[2] P. Dubey, V. Shrivastav, P.H. Maheshwari, S. Sundriyal, Recent advances in biomass derived activated carbon electrodes for hybrid electrochemical capacitor applications: challenges and opportunities, Carbon 170 (2020) 1–29, https://doi.org/10.1016/j.carbon.2020.07.056.

[3] F. Yao, D.T. Pham, Y.H. Lee, Carbon-based materials for Lithium-ion batteries, electrochemical capacitors, and their hybrid devices, ChemSusChem 8 (2015) 2284–2311, https://doi.org/10.1002/cssc.201403490.

[4] A. Abdisattar, M. Yeleuov, C. Daulbayev, K. Askaruly, A. Tolynbekov, A. Taurbekov, N. Prikhodko, Recent advances and challenges of current collectors for supercapacitors, Electrochem. Commun. 142 (2022) 107373, https://doi.org/10.1016/j.elecom.2022.107373.

[5] Y. Wang, Z. Shi, Y. Huang, Y. Ma, C. Wang, M. Chen, Y. Chen, Supercapacitor devices based on graphene materials, J. Phys. Chem. C 113 (2009) 13103–13107, https://doi.org/10.1021/jp902214f.

[6] A. Gopalakrishnan, C.Y. Kong, S. Badhulika, Scalable, large-area synthesis of heteroatom-doped few-layer graphene-like microporous carbon nanosheets from biomass for high-capacitance supercapacitors, New J. Chem. 43 (2019) 1186–1194, https://doi.org/10.1039/C8NJ05128C.

[7] X. He, P. Ling, M. Yu, X. Wang, X. Zhang, M. Zheng, Rice husk-derived porous carbons with high capacitance by ZnCl2 activation for supercapacitors, Electrochim. Acta 105 (2013) 635–641, https://doi.org/10.1016/j.electacta.2013.05.050.

[8] C. Yuan, H. Lin, H. Lu, E. Xing, Y. Zhang, B. Xie, Synthesis of hierarchically porous MnO2/rice husks derived carbon composite as high-performance electrode material for supercapacitors, Appl. Energy 178 (2016) 260–268, https://doi.org/10.1016/j.apenergy.2016.06.057.

[9] H. Fu, L. Chen, H. Gao, X. Yu, J. Hou, G. Wang, F. Yu, H. Li, C. Fan, Y. Shi, X. Guo, Walnut shell-derived hierarchical porous carbon with high performances for electrocatalytic hydrogen evolution and symmetry supercapacitors, Int. J. Hydrogen Energy 45 (2020) 443–451, https://doi.org/10.1016/j.ijhydene.2019.10.159.

[10] G. Huang, Y. Wang, T. Zhang, X. Wu, J. Cai, High-performance hierarchical N-doped porous carbons from hydrothermally carbonized bamboo shoot shells for symmetric supercapacitors, J. Taiwan Inst. Chem. Eng. 96 (2019) 672–680, https://doi.org/10.1016/j.jtice.2018.12.024.

[11] Y. Li, Z. Li, B. Xing, H. Li, Z. Ma, W. Zhang, P. Reubroycharoen, S. Wang, Green conversion of bamboo chips into high-performance phenol adsorbent and supercapacitor electrodes by simultaneous activation and nitrogen doping, J. Anal. Appl. Pyrol. 155 (2021) 105072, https://doi.org/10.1016/j.jaap.2021.105072.

[12] X. Song, X. Ma, Y. Li, L. Ding, R. Jiang, Tea waste derived microporous active carbon with enhanced double-layer supercapacitor behaviors, Appl. Surf. Sci. 487 (2019) 189–197, https://doi.org/10.1016/j.apsusc.2019.04.277.

[13] Y. Liu, X. Wang, X. Jiang, X. Li, L. Yu, Shape-controlled synthesis of porous carbons for flexible asymmetric supercapacitors, Nanoscale 10 (2018) 22848–22860, https://doi.org/10.1039/C8NR06966B.

[14] Y. Zhu, H. Hu, W. Li, X. Zhang, Resorcinol-formaldehyde based porous carbon as an electrode material for supercapacitors, Carbon 45 (2007) 160–165, https://doi.org/10.1016/j.carbon.2006.07.010.

[15] H. Wang, Z. Xu, A. Kohandehghan, Z. Li, K. Cui, X. Tan, T.J. Stephenson, C.K. King'ondu, C.M.B. Holt, B.C. Olsen, J.K. Tak, D. Harfield, A.O. Anyia, D. Mitlin, Interconnected carbon nanosheets derived from hemp for ultrafast supercapacitors with high energy, ACS Nano 7 (2013) 5131–5141, https://doi.org/10.1021/nn400731g.

[16] C.M. Ashraf, K.M. Anilkumar, B. Jinisha, M. Manoj, V.S. Pradeep, S. Jayalekshmi, Acid washed, steam activated, coconut shell derived carbon for high power supercapacitor applications, J. Electrochem. Soc. 165 (2018) A900–A909, https://doi.org/10.1149/2.0491805jes.

[17] B. Liu, L. Zhang, P. Qi, M. Zhu, G. Wang, Y. Ma, X. Guo, H. Chen, B. Zhang, Z. Zhao, B. Dai, F. Yu, Nitrogen-Doped banana peel–derived porous carbon foam as binder-free electrode for supercapacitors, Nanomaterials 6 (2016) 18, https://doi.org/10.3390/nano6010018.

[18] M.S. Balathanigaimani, W.-G. Shim, M.-J. Lee, C. Kim, J.-W. Lee, H. Moon, Highly porous electrodes from novel corn grains-based activated carbons for electrical double layer capacitors, Electrochem. Commun. 10 (2008) 868–871, https://doi.org/10.1016/j.elecom.2008.04.003.

[19] M.D. Mehare, A.D. Deshmukh, S.J. Dhoble, Preparation of porous agro-waste-derived carbon from onion peel for supercapacitor application, J. Mater. Sci. 55 (2020) 4213–4224, https://doi.org/10.1007/s10853-019-04236-7.

[20] N.M. Musyoka, B.K. Mutuma, N. Manyala, Onion-derived activated carbons with enhanced surface area for improved hydrogen storage and electrochemical energy application, RSC Adv. 10 (2020) 26928–26936, https://doi.org/10.1039/D0RA04556J.

[21] A. Gopalakrishnan, S. Badhulika, From onion skin waste to multi-heteroatom self-doped highly wrinkled porous carbon nanosheets for high-performance supercapacitor device, J. Energy Storage 38 (2021) 102533, https://doi.org/10.1016/j.est.2021.102533.

[22] M.D. Stoller, R.S. Ruoff, Best practice methods for determining an electrode material's performance for ultracapacitors, Energy Environ. Sci. 3 (2010) 1294, https://doi.org/10.1039/c0ee00074d.

[23] J. Hou, K. Jiang, R. Wei, M. Tahir, X. Wu, M. Shen, X. Wang, C. Cao, Popcorn-derived porous carbon flakes with an ultrahigh specific surface area for superior performance supercapacitors, ACS Appl. Mater. Interfaces 9 (2017) 30626–30634, https://doi.org/10.1021/acsami.7b07746.

[24] L. Stobinski, B. Lesiak, A. Malolepszy, M. Mazurkiewicz, B. Mierzwa, J. Zemek, P. Jiricek, I. Bieloshapka, Graphene oxide and reduced graphene oxide studied by the XRD, TEM and electron spectroscopy methods, J. Electron. Spectrosc. Relat. Phenom. 195 (2014) 145–154, https://doi.org/10.1016/j.elspec.2014.07.003.

[25] An Lee, Kim Park, Mesopore-rich activated carbons for electrical double-layer capacitors by optimal activation condition, Nanomaterials 9 (2019) 608, https://doi.org/10.3390/nano9040608.

[26] M. Yeleuov, C. Daulbayev, A. Taurbekov, A. Abdisattar, R. Ebrahim, S. Kumekov, N. Prikhodko, B. Lesbayev, K. Batyrzhan, Synthesis of graphene-like porous carbon from biomass for electrochemical energy storage applications, Diam. Relat. Mater. 119 (2021) 108560, https://doi.org/10.1016/j.diamond.2021.108560.

[27] M. Yeleuov, C. Seidl, T. Temirgaliyeva, A. Taurbekov, N. Prikhodko, B. Lesbayev, F. Sultanov, C. Daulbayev, S. Kumekov, Modified activated graphene-based carbon electrodes from rice husk for supercapacitor applications, Energies 13 (2020) 4943, https://doi.org/10.3390/en13184943.

[28] Y. Bleu, F. Bourquard, A. Loir, V. Barnier, F. Garrelie, C. Donnet, Raman study of the substrate influence on graphene synthesis using a solid carbon source via rapid thermal annealing, J. Raman Spectrosc. 50 (2019) 1630–1641, https://doi.org/10.1002/jrs.5683.

[29] K. Askaruly, A.V. Korobeinyk, S. Azat, M. Yeleuov, A. Taurbekov, K. Toshtay, Z. Tauanov, X. Su, The electrochemical behavior of silica and activated carbon materials derived from the rice husk waste for li-ion cells, Diam. Relat. Mater. 133 (2023) 109759, https://doi.org/10.1016/j.diamond.2023.109759.

[30] A.C. Ferrari, Raman spectroscopy of graphene and graphite: disorder, electron–phonon coupling, doping and nonadiabatic effects, Solid State Commun. 143 (2007) 47–57, https://doi.org/10.1016/j.ssc.2007.03.052.

[31] L.L. Zhang, X.S. Zhao, Carbon-based materials as supercapacitor electrodes, Chem. Soc. Rev. 38 (2009) 2520, https://doi.org/10.1039/b813846j.

[32] Q. Ke, J. Wang, Graphene-based materials for supercapacitor electrodes – a review, Journal of Materiomics 2 (2016) 37–54, https://doi.org/10.1016/j.jmat.2016.01.001.

[33] J. Pallarés, A. González-Cencerrado, I. Arauzo, Production and characterization of activated carbon from barley straw by physical activation with carbon dioxide and steam, Biomass Bioenergy 115 (2018) 64–73, https://doi.org/10.1016/j.biombioe.2018.04.015.

[34] A. Laheäär, P. Przygocki, Q. Abbas, F. Béguin, Appropriate methods for evaluating the efficiency and capacitive behavior of different types of supercapacitors, Electrochem. Commun. 60 (2015) 21–25, https://doi.org/10.1016/j.elecom.2015.07.022.
[35] H. Heydari, S.E. Moosavifard, M. Shahraki, S. Elyasi, Facile synthesis of nanoporous CuS nanospheres for high-performance supercapacitor electrodes, J. Energy Chem. 26 (2017) 762–767, https://doi.org/10.1016/j.jechem.2017.03.007.
[36] M. Usha Rani, K. Nanaji, T.N. Rao, A.S. Deshpande, Corn husk derived activated carbon with enhanced electrochemical performance for high-voltage supercapacitors, J. Power Sources 471 (2020) 228387, https://doi.org/10.1016/j.jpowsour.2020.228387.
[37] K. Nanaji, U.V. Varadaraju, T.N. Rao, S. Anandan, Robust, Environmentally Benign Synthesis of Nanoporous Graphene Sheets from Bio-Waste for Ultrafast Supercapacitor Application, (n.d.).
[38] T. Mitravinda, K. Nanaji, S. Anandan, A. Jyothirmayi, V.S.K. Chakravadhanula, C.S. Sharma, T.N. Rao, Facile synthesis of corn silk derived nanoporous carbon for an improved supercapacitor performance, J. Electrochem. Soc. 165 (2018) A3369–A3379, https://doi.org/10.1149/2.0621814jes.
[39] D. Bhattacharjya, J.-S. Yu, Activated carbon made from cow dung as electrode material for electrochemical double layer capacitor, J. Power Sources 262 (2014) 224–231, https://doi.org/10.1016/j.jpowsour.2014.03.143.
[40] X. You, M. Misra, S. Gregori, A.K. Mohanty, Preparation of an Electric Double Layer Capacitor (EDLC) Using Miscanthus-Derived Biocarbon, (n.d.).
[41] X. Wang, Y. Li, F. Lou, M.E. Melandsø Buan, E. Sheridan, D. Chen, Enhancing capacitance of supercapacitor with both organic electrolyte and ionic liquid electrolyte on a biomass-derived carbon, RSC Adv. 7 (2017) 23859–23865, https://doi.org/10.1039/C7RA01630A.
[42] Y.-H. Chiu, L.-Y. Lin, Effect of activating agents for producing activated carbon using a facile one-step synthesis with waste coffee grounds for symmetric supercapacitors, J. Taiwan Inst. Chem. Eng. 101 (2019) 177–185, https://doi.org/10.1016/j.jtice.2019.04.050.
[43] A. Gopalakrishnan, A. Yu, S. Badhulika, Facile synthesis of highly porous N-doped carbon nanosheets with silica nanoparticles for ultrahigh capacitance supercapacitors, Energy Fuels 34 (2020) 11508–11518, https://doi.org/10.1021/acs.energyfuels.0c02078.
[44] Y. Ma, J. Yin, H. Liang, D. Yao, Y. Xia, K. Zuo, Y.-P. Zeng, A two step approach for making super capacitors from waste wood, J. Clean. Prod. 279 (2021) 123786, https://doi.org/10.1016/j.jclepro.2020.123786.